Concentration dependence of self-interstitial and boron diffusion in silicon

Wolfgang Windl[a)]
Materials Science and Engineering, The Ohio State University, Columbus, Ohio 43210-1178, USA

(Received 11 April 2008; accepted 2 May 2008; published online 19 May 2008)

We show that recent experimental data and *ab initio* calculations agree on the charge state as a function of the Fermi energy of the dominant species for diffusion of self-interstitials (+, +, and 0) and boron atoms (+) in silicon. By mapping the experimental data onto the activation energy versus Fermi-level representation commonly used to display *ab initio* results, we can show that the experimental results are consistent with each other. While theoretical values for the boron activation energy as a function of the Fermi level agree well with experiment, values for self-interstitials are low, despite using total-energy corrections. © *2008 American Institute of Physics*.
[DOI: 10.1063/1.2936081]

The diffusion mechanism of boron has not been understood for a very long time despite considerable research interest.[1] It is widely accepted by now that boron diffuses nearly exclusively with the help of Si self-interstitials (*I*'s).[2] That is, the mobile entity is thought to be a B atom paired with an *I*. Concerning the diffusion mechanism, Windl *et al.* used the nudged elastic band method[3] within density-functional theory[4] to examine the minimum-energy barrier diffusion path for *I*-assisted, charge-state dependent B diffusion within both the local density approximation (LDA) and the generalized-gradient approximation (GGA), and found a kick-in/kick-out mechanism, following a number of previous studies with varying results.[5] Although this work has been performed several years ago, recent experiments by De Salvador *et al.*[6] and Bracht *et al.*[7] have re-examined the charge states of both the boron atom and interstitials involved, which we use to re-evaluate the simulation results.

Especially interesting is the simultaneous measurement of the interaction rate g between B and I and the mean free path λ as a function of hole concentration p in Ref. 6, which are related to the diffusivity D by $D=g\lambda^2$.[8,9] In thermodynamic equilibrium in a homogenous material, the impurity transport can be described by[8]

$$\partial C_{\mathrm{B}I}/\partial t = D_{\mathrm{B}I}\nabla^2 C_{\mathrm{B}I} - rC_{\mathrm{B}I} + gC_{\mathrm{B}_s}, \tag{1}$$

$$\partial(C_{\mathrm{B}_s} + C_{\mathrm{B}I})/\partial t = D_{\mathrm{B}I}\nabla^2 C_{\mathrm{B}I}, \tag{2}$$

where C_{B_s} and $C_{\mathrm{B}I}$ are the concentrations of the ground state, substitutional boron B_s, and the mobile boron interstitial pair, BI. Since for B diffusion in Si the kick-out mechanism dominates ($\mathrm{B}_s + I \rightarrow \mathrm{B}I$),[5] the generation rate g is given by the forward reaction rate[10] of the kick-out mechanism times self-interstitial concentration,

$$g = 4\pi a_c^{\mathrm{B}I} D_I C_I, \tag{3}$$

where $a_c^{\mathrm{B}I}$ is the B-I capture radius. g is thus directly proportional to the self-interstitial transport coefficient, D_IC_I. Since $\lambda=\sqrt{D/g}$,[8,9] we get overall

$$D_{\mathrm{B}} = D_{\mathrm{B}0}\exp(-\beta E_a^{\mathrm{B}}), \tag{4}$$

$$g = 4\pi a_c^{\mathrm{B}I}(D_IC_I)_0\exp(-\beta E_a^I), \tag{5}$$

$$\lambda = \sqrt{\frac{D_{\mathrm{B}0}}{4\pi a_c^{\mathrm{B}I}(D_IC_I)_0}}\exp\left[-\beta\frac{E_a^{\mathrm{B}} - E_a^I}{2}\right], \tag{6}$$

where $\beta=1/(k_BT)$. Since calculated values for all energies and the capture radius $a_c^{\mathrm{B}I}$ exist, we will first report the results of those calculations and then compare them to the recent experimental results in Refs. 6 and 7.

Equations (4)–(6) are controlled by the activation energies for B and I diffusion. 216-atom, $2\times2\times2$ k-point GGA calculations for the Si self-interstitial with the corrections discussed in Ref. 11 suggest that only tetrahedral T^{++} and split-interstitial X^0 are stable (the midgap formation energies are 3.74 and 3.70 eV, respectively), whereas T^+ and negative charge states have the lowest energy for no Fermi level position. For the migration energies, we find values of 1.03, 0.02, and 1.14 eV for X^0, T^+, and T^{++}, respectively. Although the barrier for T^+ diffusion looks very small, experiments have suggested that self-interstitials in Si are mobile at temperatures of 4.2 K (Ref. 12) and even at 0.5 K,[13] which would be the easiest for a small migration barrier such as the one found for + charge. The activation energy for the transport coefficient C_ID_I at midgap is given by 4.73, 4.32, and 4.88 eV for X^0, T^+, and T^{++}, respectively, making T^+ the dominant mobile species. These values are somewhat lower than the measured values of 4.96, 4.82, and 5.02 eV in Ref. 7, extracted from dopant and self-diffusion experiments in Si isotope multilayer structures, but are of the same trend, $E_a^+ < E_a^0 < E_a^{++}$.

The results for the energetics of interstitial-assisted boron diffusion have been published in Ref. 5. These activation energies from LDA and GGA calculations, along with experimental data, are shown in Fig. 1. Also, Beardmore *et al.*[14] calculated the BI capture radius $a_c^{\mathrm{B}I}$ from kinetic Monte Carlo simulations based on *ab initio* calculated interaction energies up to the 11th neighbor shell to be 4.6 Å at 900 °C. Assuming a similar temperature dependence as found in Ref. 14 for AsV and PV, the capture radius for BI at 700 °C might be somewhat higher, around 5.4 Å. However, due to the lack of hard data, we use in the following section the 900 °C value of 4.6 Å.

The results of the zero-temperature calculations described in the previous two paragraphs were reported as functions of the Fermi energy. In order to compare the experimental values from Ref. 6 with these results, it is helpful

a)Electronic mail: windl.1@osu.edu.

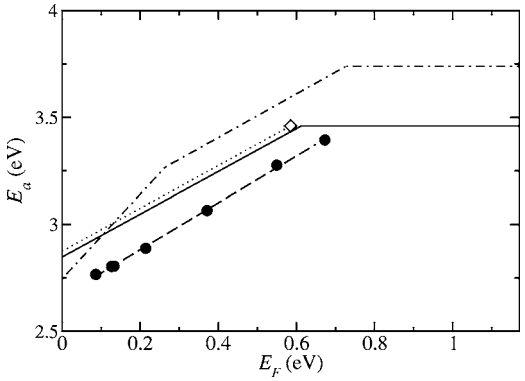

FIG. 1. Activation energy for B diffusion. Solid line for the theoretical LDA curve and dot-dashed line for the GGA curve, both from Ref. 5 (shown are only the lines for the lowest-energy charge state for clarity). The diamond is a recent experimental value from Ref. 7 and the circles represent values from Ref. 6 calculated from D vs p values, both with rescaled energies to match the high-temperature intrinsic Fermi energy to the zero-temperature value. The dashed line is a fit to the values from Ref. 6; the dotted line corresponds to the +1 slope suggested in Ref. 7.

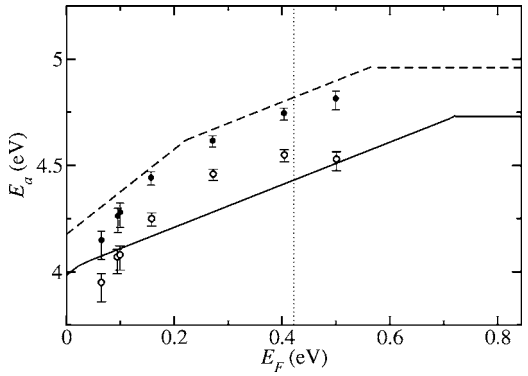

FIG. 2. Calculated activation energy for the generation rate (and thus Si self-interstitial transport coefficient) scaled to the high-temperature band gap with fixed intercepts (solid line) from an analysis of dopant and self-diffusion in silicon isotope multilayer structures (dashed line) (Ref. 7) and calculated according to Eq. (7) from the values for the generation rate in Ref. 6 with either an averaged prefactor from Ref. 7 (empty circles) or the Fermi-level-dependent prefactor from Eq. (8) (full circles).

to define the dependence of Eqs. (4)–(6) on the hole concentration, p, in a somewhat unusual form by allowing a concentration dependence of prefactor and activation energy. For the example of the diffusion constant, this results in $D(p)=D_0(p)\exp[-\beta E_a(p)]$ and thus

$$E_a(p) = -k_B T \ln[D(p)/D_0(p)] \tag{7}$$

(with analogous expressions for g and λ, respectively). Thus, $E_a(p)$ can be calculated, provided a value/function for the prefactor $D_0(p)$ is available. To plot E_a as a function of the Fermi level E_F instead of p, we use the familiar $E_F(p)=E_F^i - k_B T \ln(p/n_i)$. For the necessary parameters to convert the experimental results of Ref. 6 at 700 °C, we use[15] $n_i=1.0\times10^{18}$ cm^{-3} and $E_F^i=E_g/2+\frac{3}{4}\ln(m_p^*/m_n^*)=0.42$ eV (using Thurmonds' expression[16] for E_g and Jain and Van Overstraeten's effective masses[17] m^*).

Variations in D_0 with Fermi energy, as are typically present in the widely used expression $D=D^0+(p/n_i)D^+ +\cdots$, are not important for boron diffusion, which is dominated by a single charge state, but have to be taken into account for self-interstitials. For the interstitial prefactor $(C_I D_I)_0$, which depends on the charge state Q, we use a Boltzmann average with Fermi-level-dependent activation energies,

$$D_0^I(E_F) = \frac{\sum_{Q=0}^{2} D_0^I(Q) e^{\{-\beta[E_a^I(Q)+Q(E_F-E_F^i)]\}}}{\sum_{Q=0}^{2} e^{\{-\beta[E_a^I(Q)+Q(E_F-E_F^i)]\}}}, \tag{8}$$

with $D_0^I(0)=2732$ cm^2/s, $D_0^I(1)=69.9$ cm^2/s, $D_0^I(2)=469$ cm^2/s, $E_a^I(0)=4.96$ eV, $E_a^I(1)=4.82$ eV, and $E_a^I(2)=5.02$ eV.[7] For B, we use $D_{B0}=0.87$ cm^2/s.[7]

In Fig. 1, we show the theoretical activation energies from LDA and GGA calculations as a function of the Fermi energy from Ref. 5. Also, we include the experimental data from Refs. 6 and 7. The energies of Ref. 6 have been determined from D versus p data according to the above described procedure. There is some uncertainty concerning the necessary prefactor D_0 [Eq. (7)], which we assumed to be equal to the most recent value of 0.87 cm^2/s.[7] Among the different possibilities to scale the experimental high-temperature activation energies to 0 K in the absence of experimental data for the temperature dependence of the ionization energies, we chose to maintain at zero temperature the value of the experimental high-temperature activation energy at the intrinsic Fermi level and its slope. For this, we used $E_F^{0\ \mathrm{K}}(p)=(E_F^{i,0\ \mathrm{K}}/E_F^{i,\mathrm{HT}})E_F^{\mathrm{HT}}(p)$ and $E_a^{0\ \mathrm{K}}[E_F^{0\ \mathrm{K}}(p)]=E_a^{\mathrm{HT}}(E_F^{i,\mathrm{HT}})-(E_F^{i,0\ \mathrm{K}}/E_F^{i,\mathrm{HT}})\{E_a^{\mathrm{HT}}(E_F^{i,\mathrm{HT}})-E_a^{\mathrm{HT}}[E_F^{\mathrm{HT}}(p)]\}$.

The values from Ref. 6 are lower than both LDA and GGA results, whereas the value from Ref. 7 is higher at 3.46 eV (midgap) and is very close especially to the LDA result. Independent of this, the most important result of the carrier-concentration-dependent diffusivity values from Ref. 6 is the shape of the underlying curve. It is straight with a fitted slope of 1.09 (close to the expected value of 1) and extends into the n-type regime, which was experimentally achieved by counterdoping with phosphorus. Reference 7 comes to the same conclusion. This behavior is in agreement with the theoretical LDA curve in the p regime, which predicts a diffusion coefficient proportional to p/n_i in that region. Although it extends this behavior into the n-type regime, the theoretical p/n_i regime ends at a lower Fermi energy than experiment. This situation might be different when scaling the calculations to high temperatures with potential ionization-energy shifts, which we did not attempt. The GGA curve displays higher values with larger discrepancies with experiment and shows a $(p/n_i)^2$ behavior for Fermi energies close to the valence band edge (i.e., high p-type doping), different from the experimental curve. On the other hand, its linear regime extends to higher Fermi energy values, in agreement with experiment.

According to Eq. (3), the generation rate g is proportional to the self-interstitial transport coefficient. We can thus use an equation analogous to Eq. (7) to extract the activation energy for Si interstitial diffusion from the g results of Ref. 6, provided we know the prefactor for the I transport coefficient and the capture radius for the BI reaction. For the latter, we take the value of 4.6 Å from Ref. 14; for the former, we use Eq. (8) with the values from Ref. 7. To demonstrate the influence of the prefactor, we also use a constant Fermi-level-independent prefactor from averaging the values from Ref. 7. Figure 2 shows the results of this procedure in comparison to the theoretical activation energies and the results from Ref. 7. For this comparison with the theoretical calculations, the latter have been scaled to the 700 °C bandgap, leaving the relative ionization levels fixed.

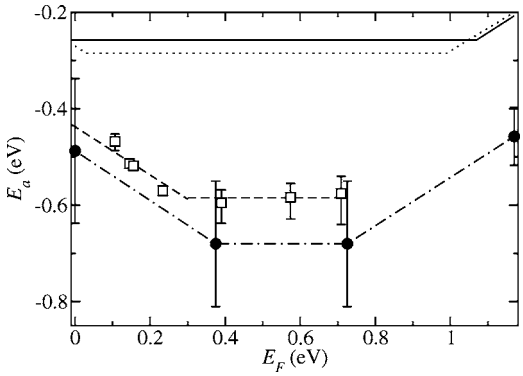

FIG. 3. Activation energy for the mean free path. The solid (dotted) lines are calculated from one-half the difference between boron and self-interstitial activation energies determined within LDA (GGA) calculations. The solid dots and dot-dashed lines are calculated from the corresponding experimental values from Ref. 7. The open squares are calculated according to Eq. (7) from the values for the mean free path in Ref. 6 using the Fermi-level-dependent prefactor from Eq. (8).

The theoretical GGA results and the values from Ref. 7 agree in the sense that they both predict I^0, I^+, and I^{++} as dominant mobile species, depending on the Fermi level. The low theoretical value for the activation energy of I^+ (T^+) causes the ionization energies to be close to the band edges. Using the constant prefactor, the experimental points from Ref. 6 follow a parabolic shape (open circles in Fig. 2), similar to the plot against p/n_i in Ref. 6, which could then be fitted with a constant and a plus-2 term. However, when using the Fermi-level-dependent prefactor from Eq. (8), one can clearly distinguish two linear regions with different slopes of potentially ~ 1 and ~ 2 (with the exception of the point closest to the valence band edge, which is somewhat lower). Thus, from this picture, one could argue that the slopes for single and double positive charge states of the self-interstitial can be seen. The activation energies extracted from the generation rate are very similar to the experimental results of Ref. 7 when using the Fermi-level-dependent prefactor and are thus higher than the calculated results, and vice versa when using the constant prefactor.

As shown in Eq. (6), the mean free path λ can be calculated from the boron diffusion and self-interstitial transport coefficients as well as the B-I capture radius. Its energy dependence is given by one-half the difference between the activation energies for boron and self-interstitial transport. In order to extract the energy dependence of the mean free path data in Ref. 6, we use Eq. (7) along with Eq. (6) to define the necessary prefactor from the data described above. The prefactor for self-interstitial transport is again calculated as a function of the Fermi level using Eq. (8).

Figure 3 shows clearly a slope of $-\frac{1}{2}$ in the p^+ regime and zero closer to midgap. Considering Eq. (6), this is consistent with the slopes for boron and self-interstitial diffusion in Figs. 1 and 2. The extracted energies are once again in excellent agreement with the findings of Ref. 7. Since the *ab initio* energies agree well with experiment in the case of boron, but seem to be low for self-interstitials, it is not surprising that their difference is considerably higher than both experimental results. However, the calculated charge states are once again in agreement with experiment.

In summary, we have used *ab initio* calculations for I and B diffusion in Si and recent experimental data[6,7] to study the Fermi-level dependence of self-interstitial and B diffusion in Si. Mapping the experimental data onto the activation energy versus Fermi-level representation commonly used to display *ab initio* results, the experimental results are consistent with each other. The theoretical activation energy for boron diffusion as a function of the Fermi level[5] agrees well with experiment. For the self-interstitial, we find in line with other calculations an underestimation of the experimental values, despite using total-energy corrections. Since the predicted activation energies not only for boron but also for other interstitial diffusers is, in general, predicted much closer to experiment than the self-interstitial energies,[18–20] it might indeed be plausible that point-defect interactions and reactions could be the reason for the discrepancy between experiment and theory, as previously speculated in Ref. 7.

[1] P. Pichler, *Intrinsic Point Defects, Impurities, and Their Diffusion in Silicon* (Springer, Berlin, 2004), Chap. 1.5.
[2] A. Ural, P. B. Griffin, and J. D. Plummer, J. Appl. Phys. **85**, 6440 (1999).
[3] H. Jónsson, G. Mills, and K. W. Jacobsen, in *Classical and Quantum Dynamics in Condensed Phase Simulations*, edited by B. J. Berne, G. Ciccotti, and D. F. Coker (World Scientific, Singapore, 1998), p. 385.
[4] G. Kresse and J. Hafner, Phys. Rev. B **47**, 558 (1993); **49**, 14 251 (1994); J. Phys.: Condens. Matter **6**, 8245 (1994); G. Kresse and J. Furthmüller, Comput. Mater. Sci. **6**, 15 (1996); Phys. Rev. B **54**, 11 169 (1996).
[5] W. Windl, M. M. Bunea, R. Stumpf, S. T. Dunham, and M. P. Masquelier, Phys. Rev. Lett. **83**, 4345 (1999).
[6] D. De Salvador, E. Napolitani, S. Mirabella, G. Bisognin, G. Impellizzeri, A. Carnera, and F. Priolo, Phys. Rev. Lett. **97**, 255902 (2006).
[7] H. Bracht, H. H. Silvestri, I. D. Sharp, and E. E. Haller, Phys. Rev. B **75**, 035211 (2007).
[8] N. E. B. Cowern, K. T. F. Janssen, G. F. A. van de Walle, and D. J. Gravesteijn, Phys. Rev. Lett. **65**, 2434 (1990).
[9] N. E. B. Cowern, G. F. A. van de Walle, D. J. Gravesteijn, and C. J. Vriezema, Phys. Rev. Lett. **67**, 212 (1991).
[10] T. R. Waite, Phys. Rev. **107**, 463 (1957).
[11] W. Windl, Phys. Status Solidi B **241**, 2313 (2004).
[12] G. D. Watkins, *Radiation Damage in Semiconductors* (Dunod, Paris, 1964), p. 97.
[13] P. S. Gwozdz and J. S. Köhler, Phys. Rev. B **6**, 4571 (1972).
[14] K. M. Beardmore, W. Windl, B. P. Haley, and N. Grønbech-Jensen, *Computational Nanoscience and Nanotechnology 2002* (Applied Computational Research Society, Cambridge, 2002), p. 251.
[15] F. J. Morin and J. P. Maita, Phys. Rev. **96**, 28 (1954).
[16] C. D. Thurmond, J. Electrochem. Soc. **122**, 1133 (1975).
[17] R. K. Jain and R. J. Van Overstraeten, IEEE Trans. Electron Devices **ED-21**, 155 (1974).
[18] N. G. Stoddard, P. Pichler, G. Duscher, and W. Windl, Phys. Rev. Lett. **95**, 025901 (2005).
[19] C. L. Liu, W. Windl, L. Borucki, S. F. Lu, and X. Y. Liu, Appl. Phys. Lett. **80**, 52 (2002).
[20] X. Y. Liu, W. Windl, K. M. Beardmore, and M. P. Masquelier, Appl. Phys. Lett. **82**, 1839 (2003).